calculation with simple trial functions and only four parameters.

(3) The potential used in the calculation is weak, providing an extreme test for a local-orbital picture.

We feel these are encouraging results. They imply that the GWF formalism will provide a practical, efficient calculational technique for solid surfaces. We believe this to be especially important for transition metals and their oxides. For these, one must deal with a mixture of contracted and diffuse orbitals immersed in the inhomogeneous medium of the surface. A method which represents surface observables precisely in terms of local functions is ideally suited to this problem.

The authors would like to thank W. Kohn, E. W. Plummer, G. G. Kleiman, F. A. Arlinghaus, and J. C. Tracy for helpful conversations. Programming assistance from J. C. Price is gratefully acknowledged.

[1]The evidence is especially apparent in recent experiments on the elemental semiconductors. Ion-neutralization spectroscopy, which probes essentially only the surface layer of atoms, gives electron energy distributions which are qualitatively different from the bulk density of states [H. B. Hagstrum and G. E. Becker, Phys. Rev. B 8, 1580 (1973)], whereas in ultraviolet photoemission spectroscopy, the electron energy distributions are dominated by the bulk density of states even under conditions in which the experiment probes only about four atom layers [D. E. Eastman and W. D. Grobman, Phys. Rev. Lett. 28, 1378 (1972)].

[2]W. Kohn and J. Onffroy, Phys. Rev. B 8, 2485 (1973).

[3]J. G. Gay and J. R. Smith, Phys. Rev. B (to be published).

[4]W. Kohn, Phys. Rev. B 1, 4388 (1973).

[5]P. O. Löwdin, J. Chem. Phys. 18, 365 (1950).

[6]J. D. Weeks, P. W. Anderson, and A. G. H. Davidson, J. Chem. Phys. 58, 1388 (1973).

[7]P. M. Morse and H. Feshbach, *Methods of Theoretical Physics* (McGraw-Hill, New York, 1953), Pt. II, p. 1650.

[8]J. C. Slater, *Symmetry and Energy Bands in Crystals* (Dover, New York, 1972), Chap. 6. The Mathieu potential used corresponds to a value of 1 for Slater's parameter s.

[9]J. C. Slater, Phys. Rev. 87, 807 (1952).

Angular Distributions of Electron-Stimulated–Desorption Ions: Oxygen on W(100)

Jerzy J. Czyzewski,* Theodore E. Madey, and John T. Yates, Jr.
Surface Chemistry Section, National Bureau of Standards, Washington, D. C. 20234
(Received 22 January 1974)

Ions liberated from an adsorbed layer by electron-stimulated desorption are shown to have sharply peaked, symmetric angular distributions which are in registry with the substrate. We propose a new method for investigation of the symmetry of binding sites for adsorbed species.

Low-energy electron (~100 eV) bombardment of a surface containing an adsorbed layer can produce a number of irreversible changes in the adsorbed layer. The electron-induced desorption of atomic and molecular ions, neutrals, and metastable species from monolayer and submonolayer quantities of simple gases adsorbed on metal and semiconductor surfaces has been observed. These processes are all classified as electron-stimulated desorption (ESD) phenomena.[1] In a recent ESD study of oxygen adsorbed on a single-crystal tungsten (100) surface, evidence was found that O^+ ions liberated from the surface had an angular distribution which was sharply peaked in the direction normal to the surface.[2]

In the present report, we have employed a display-type apparatus to examine the details of the angular distribution of O^+ ions in an ESD study of oxygen on W(100). Surprisingly, the angular distributions of ESD ions reveal complex symmetrical patterns in registry with the substrate lattice which change as a function of the oxygen coverage and heat treatment of the surface. We propose that the symmetry observed in the patterns for the angular distributions of ESD ions provides new insights into the details of bonding of atoms and molecules at surfaces.

In the experimental ultrahigh-vacuum apparatus, an electron gun was used to bombard a W(100) crystal with a focused electron beam at a 45° angle of incidence. Ions liberated from the crystal passed through a hemispherical grid system and were accelerated to a planar microchannel plate assembly.[3] The secondary-electron signal

from the microchannel plates was displayed visually by acceleration of the electrons to a phosphor-coated screen. In order to minimize ESD damage by the electron beam, electron currents were typically 1×10^{-10} to 5×10^{-9} A. By appropriate biasing of the grids and microchannel plates, the apparatus was also used to provide a visual display of the elastic low-energy electron diffraction (LEED) pattern from the surface. Switching from angular distributions of ESD ions to the LEED mode was accomplished in a few seconds, so that both techniques were used to characterize the state of the adsorbed layer.

The crystal was cleaned in vacuum at temperatures >2500 K by electron bombardment from an auxiliary tungsten filament mounted behind the crystal. This filament was also used to heat the crystal by radiation to temperatures up to ~1100 K. Temperatures were measured using both an optical pyrometer and a W/W–26% Re thermocouple spot welded to the crystal. High-purity oxygen was admitted to the vacuum system via a variable leak. Pressures were read on an uncalibrated Bayard-Alpert ionization gauge which was turned off during the later stages of each oxygen dose.

Before discussing the results for angular distributions of ESD ions, a brief review of the O_2/W(100) system is appropriate. Based on previous ESD studies[1,2,4,5] of oxygen adsorbed on both polycrystalline and single-crystal tungsten, several generalizations can be drawn. (1) The only ionic ESD product is O^+. (2) For oxygen coverages $\lesssim 8\times10^{14}$ atoms/cm^2 on W(100), the O^+ ion yield is small, $\lesssim 5\times10^{-9}$ ion/electron. This low-ion-yield state is termed β_2 oxygen, and arises from the adsorbed species which desorb as atomic oxygen.[6] (3) For oxygen coverages $\gtrsim 8\times10^{14}$ atoms/cm^2, the ion yield is high, $\sim10^{-6}$ ion/electron. This state is termed β_1 oxygen, and has been variously attributed to an adsorbed molecular-oxygen state and to surface tungsten oxides.[1,6]

Figure 1 contains three patterns obtained by photographing the phosphor screen under different conditions. Figure 1(a) is a LEED pattern of the clean W(100) surface, which identifies the orientation of the rows of substrate atoms for comparison with the subsequent patterns for the angular distributions of ESD ions. Figure 1(b) is an ESD pattern of O^+ ions from the W(100) surface at ~300 K; the clean crystal had been exposed to an oxygen dose sufficient to produce a coverage of about 0.5 monolayer [$\sim 5\times10^{14}$ (O atoms)/cm^2] at ~400 K. The arms of the diffuse cross in this pattern are parallel to the atom rows. This pattern is characteristic of the low-coverage, low-ion-yield β_2 oxygen state, and was only visible at relatively high electron bombardment currents (10^{-8} to 10^{-7} A). Figure 1(c) is characteristic of the high-coverage, high-ion-yield β_1 oxygen state, and was observed following oxygen exposures of $\gtrsim 9\times10^{-6}$ Torr sec with the surface at temperatures $\lesssim 400$ K. The pattern of Fig. 1(c) is rotated by 45° with respect to the atom rows in the (100) crystal, and exhibits distinct circular lobes in a fourfold symmetric arrangement. The β_1 ESD pattern of Fig. 1(c) may also contain a contribution from the β_2 state [Fig. 1(b)]; however, the differences in relative ion desorption cross sections Q^+ for the two states ($Q_{\beta_1}{}^+/Q_{\beta_2}{}^+ > 100$) is so great that it is not possible to photograph simultaneously the contributions from both states.

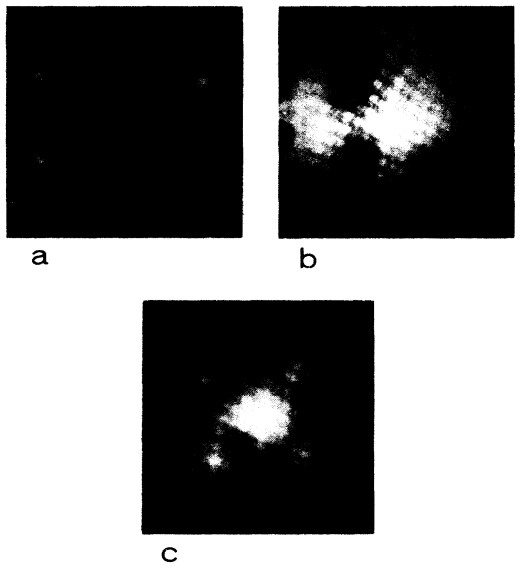

FIG. 1. (a) LEED pattern for clear W(100) surface; electron energy $V_e=123$ eV. (b) ESD pattern for low-coverage β_2 oxygen on W(100); $V_e=180$ eV, $T\lesssim400$ K. (c) ESD pattern for high-coverage β_1 oxygen on W(100); $V_e=180$ eV, $T\lesssim400$ K.

Figure 2 contains a sequence of patterns for the angular distributions of ESD O^+ which are observed following heating of the oxygen-covered surface. The crystal was first cleaned in vacuum, then exposed to 40×10^{-6} Torr sec of oxygen at $\lesssim 400$ K to populate the β_1 state. Then the crystal was heated in vacuum to increasingly higher temperatures before being cooled to photograph the

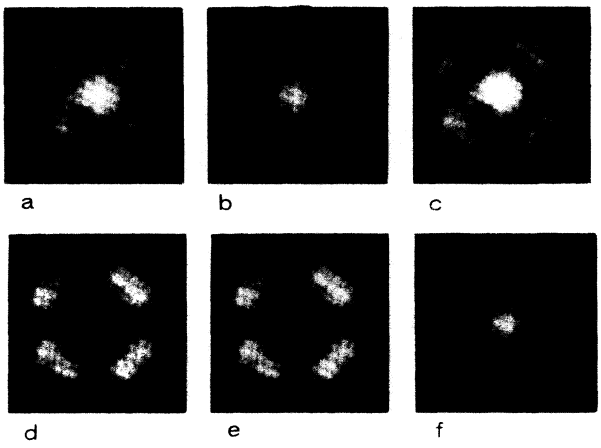

FIG. 2. Effect of heat treatment on ESD patterns for β_1 oxygen on W(100). Temperatures corresponding to each pattern are (a) $\lesssim$400 K, (b) 630 K, (c) 705 K, (d) 795 K, (e) 865 K, and (f) 930 K.

ESD pattern. The patterns of Fig. 2 were obtained following 10 sec of heating at the indicated temperature. The ESD patterns exhibit distinct changes in appearance as the surface is heated. The central spot dominates the angular distribution at $\lesssim$600 and $\gtrsim$900 K, whereas the fourfold lobes dominate the angular distribution in the intermediate temperature region. Each of the lobes in Figs. 2(c)–2(e) appears to be split, and actually consists of two partially resolved spots. At temperatures $\gtrsim$1000 K, the ion yield is very low, and the central-spot pattern gradually disappears.

All of the ESD patterns of Figs. 1 and 2 have been compressed for convenience of display using appropriate bias potentials. All of the ion emission displayed in the patterns of Figs. 1 and 2 occurred within a cone having a half-angle estimated as ~45° for ions leaving the surface in the absence of applied electric fields.

It is appropriate to consider the relationship between LEED and the angular distribution of ESD ions. It was observed that there were virtually no changes in the symmetry of the LEED patterns corresponding to most of the ESD pattern changes of Fig. 2. Elastic LEED is sensitive to the long range order in the adsorbed layer, and the resulting patterns provide information regarding the size and shape of the unit cell of the two-dimensional lattice. The LEED patterns themselves do not contain direct information regarding the nature of the binding sites on the surface, i.e., where the adatoms are bound with respect to substrate atoms. This information is, in principle, contained in an analysis of the intensity-versus-energy profiles of individual LEED beams, but the analysis is complex and has just begun to bear fruit. In contrast to LEED, ESD is sensitive to the excitation of adatoms and admolecules in their individual binding sites irrespective of long range order. Since the adatom vibrates in a three-dimensional potential "well," ESD represents a statistical sampling of atom positions within this potential well. The resulting ESD patterns directly demonstrate the symmetry of the bonding sites; a fourfold symmetric pattern for an adsorbate on the (100) surface may be due to bonding on a fourfold symmetric site, or to domains of twofold symmetry. Thus some of the ambiguity of LEED is present in the angular distribution of ESD ions as well.

The only theoretical treatment of ESD phenomena presently available is based on the one-dimensional picture proposed by Redhead[7] and Menzel and Gomer.[8] Franck-Condon excitation of a ground-state adsorbate to the repulsive part of an antibonding or ionic potential curve is followed by reneutralization and/or desorption of ions, neutrals, and metastable species. This treatment has been successful in predicting such phenomena as relative ion and neutral ESD yields, high kinetic energies (~8 eV) for desorption of ions, and the ESD isotope effect.

In order to understand the patterns of the angular distributions of ESD ions, a three-dimensional theory is necessary. A complete description should include knowledge of the spatial distribution of $|\psi_{vib}|^2$ over vibrational modes for adatoms in the ground state (initial state) as well as the spatial distribution of electronically excited species (final state). In addition, the influence of directional bonding between atom and surface, as well as the possibility of specific neutralization channels in different directions, must be considered. In the one-dimensional Franck-Condon excitation model, the ejection of ions having several electron volts of kinetic energy implies that the ion velocities are determined by the shape of the repulsive-potential curve within a few tenths of angstroms of the equilibrium adatom-surface position. Extending this picture to three dimensions, it is reasonable to assume that the shape and symmetry of the three-dimensional repulsive potential contours between ion and surface will influence the trajectories of the desorbed ions. This symmetry should be reflected in the ion angular distributions.

The possible influence on the angular distribu-

tions of ESD ions of the spatial distribution of vibrational amplitudes in the initial state can be seen as follows. Calculations of localized mode frequencies[9] of an atom bound in a central site on the bcc (100) surface suggest that the maxima in the mean-square vibrational amplitude lie parallel to the atom rows, e.g., in [010] and [001] directions. Excitation from such an initial state to a structureless final state would be expected to result in an ESD pattern with the shape of a hazy cross oriented parallel to the atom rows. It is suggestive that such a pattern is seen for low-coverage β_2 oxygen [Fig. 1(b)]. For higher oxygen coverages, the β_1 ESD pattern [Figs. 1(c) and 2(a)] is rotated by 45° indicative of a change in adsorption geometry.

The appearance of focused lobes in the patterns of Figs. 1(c) and 2 is evidence for the influence of directional bonding in the angular distribution of ESD ions. Electronic excitation of a surface species to an antibonding state may result in the desorption of ions having focused directional properties related to the ground state atom-surface bond orientation.

The effect of thermal treatment on the ESD patterns (Fig. 2) illustrates the sensitivity of the angular distribution of ESD ions to surface-bonding conditions. Flash-desorption data for O_2 adsorbed on W indicate[10] that following an exposure of 40×10^{-6} Torr sec on a W surface at 300 K, oxides of tungsten desorb at $T>1200$ K, and atomic oxygen desorbs at $T>2000$ K. Flash desorption does *not* yield information regarding the temperature of oxide formation, although adsorption experiments suggest that oxides may form as low as ~ 500 K.[10] The most dramatic changes in ESD patterns occur at temperatures (~ 600–900 K) well below the onset of oxygen or oxide desorption, and may be related to the formation of surface oxides. The symmetries and relative intensities in the lobes of ESD patterns are sensitive indicators of changes in bonding character, although detailed interpretation of these complex patterns is not possible at present.

The authors acknowledge with pleasure valuable discussions with Dr. J. W. Gadzuk and the technical assistance of Mr. A. Pararas. One of us (J.J.C.) acknowledges with gratitude the financial support of the Welch Foundation Scholarship of the International Union for Vacuum Science, Technique, and Applications, as well as the Committee on International Exchange of Persons (Senior Fulbright-Hays Program).

*Guest worker, 1973–1974. Permanent address: Institute of Experimental Physics, University of Wroclaw, Cybulskiego 36, Wroclaw, Poland.

[1]For recent reviews, see, D. Menzel, Angew. Chem. Int. Ed. Engl. 9, 255 (1970); T. E. Madey and J. T. Yates, Jr., J. Vac. Sci. Technol. 8, 525 (1971).

[2]T. E. Madey, Surface Sci. 33, 355 (1972).

[3]D. J. Ruggieri, IEEE Trans. Nucl. Sci. 19, 74 (1972).

[4]A. Benninghoven, E. Loebach, and N. Treitz, J. Vac. Sci. Technol. 9, 600 (1972).

[5]T. E. Madey and J. T. Yates, Jr., Surface Sci. 11, 327 (1968).

[6]D. A. King, T. E. Madey, and J. T. Yates, Jr., J. Chem. Soc., Faraday Trans. 1 68, 1347 (1972).

[7]P. A. Redhead, Can. J. Phys. 42, 886 (1964).

[8]D. Menzel and R. Gomer, J. Chem. Phys. 41, 3311 (1964).

[9]L. Dobrzynski and P. Masri, J. Phys. Chem. Solids 33, 1603 (1972); L. Dobrzynski, Surface Sci. 20, 99 (1970).

[10]D. A. King, T. E. Madey, and J. T. Yates, Jr., J. Chem. Phys. 55, 3236, 3247 (1971).

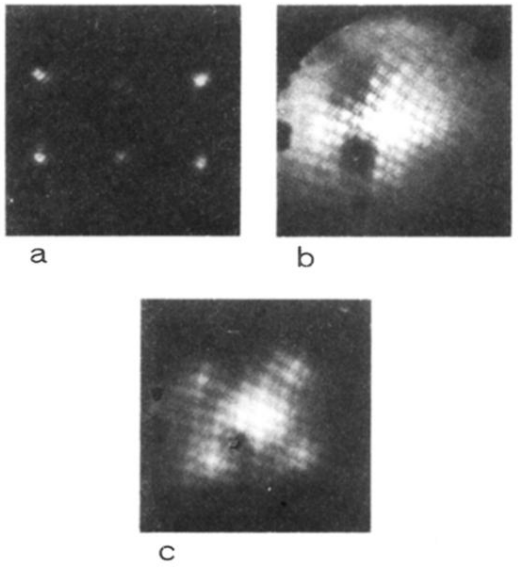

FIG. 1. (a) LEED pattern for clear W(100) surface; electron energy $V_e = 123$ eV. (b) ESD pattern for low-coverage β_2 oxygen on W(100); $V_e = 180$ eV, $T \lesssim 400$ K. (c) ESD pattern for high-coverage β_1 oxygen on W(100); $V_e = 180$ eV, $T \lesssim 400$ K.

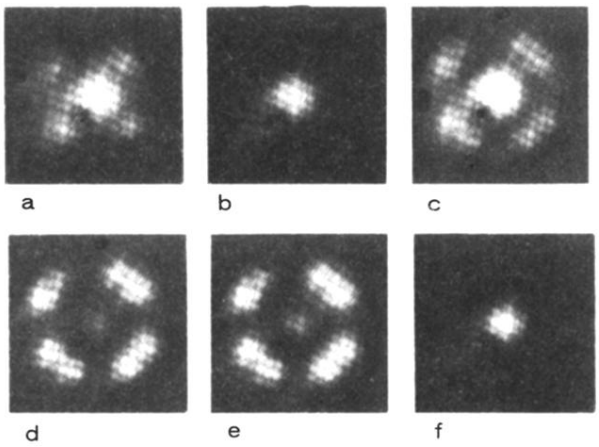

FIG. 2. Effect of heat treatment on ESD patterns for β_1 oxygen on W(100). Temperatures corresponding to each pattern are (a) $\lesssim$400 K, (b) 630 K, (c) 705 K, (d) 795 K, (e) 865 K, and (f) 930 K.